

This is the accepted manuscript made available via CHORUS. The article has been published as:

# Thermal fluctuations of the Josephson current in a ring of superconducting grains

D. A. Garanin and E. M. Chudnovsky

Phys. Rev. B **95**, 014520 — Published 24 January 2017

DOI: [10.1103/PhysRevB.95.014520](https://doi.org/10.1103/PhysRevB.95.014520)

# Thermal fluctuations of the Josephson current in a ring of superconducting grains

D. A. Garanin and E. M. Chudnovsky

*Physics Department, Lehman College and Graduate School, The City University of New York,  
250 Bedford Park Boulevard West, Bronx, NY 10468-1589, U.S.A.*

(Dated: January 12, 2017)

Thermal fluctuations of the Josephson current induced by the magnetic flux through a ring of  $N$  superconducting grains are studied. When a half-fluxon is threading the ring,  $I$  exhibits incoherent transitions between the two degenerate states due to thermal phase slips. We propose a new numerical method to deal with both equilibrium and dynamic properties of Josephson systems. Computed transition rate has the form  $\Gamma = A(N) \exp[-B(N)/T]$ , where  $B(N)$  agrees with the analytical result derived for the energy barrier associated with phase slips. In the non-degenerate case (e.g., at a quarter-fluxon) the equilibrium value of  $I$  decreases with  $T$  due to harmonic excitations and then gets destroyed by phase slips.

PACS numbers: 74.50.+r, 74.81.Fa, 73.23.Ra, 02.70.-c

## I. INTRODUCTION

Persistent currents in small metallic rings have been studied theoretically and experimentally since 1960s.<sup>1</sup> Rapid progress in manufacturing of nanostructures<sup>2</sup> has ignited a contemporary interest to measurements of microscopic chains of Josephson junctions (JJ).<sup>3</sup> Analytical studies in this area consider two limits: When the dynamics of the chain is dominated by the capacitances of the junctions<sup>4</sup> and when the dynamics is dominated by the capacitances of the superconducting islands.<sup>5</sup> Here we focus on the latter limit in the classical regime when thermal fluctuations dominate over quantum fluctuations.

There are two characteristic energy scales in the problem. One is the charging energy of the superconducting island,  $U \equiv E_C = 2e^2/C$ , where  $C$  is the capacitance of the island with respect to the ground, and the other is the Josephson energy,  $J$ . They determine the characteristic temperature ranges and physical properties of the JJ chains.<sup>5-9</sup> At  $T \ll T^* = \sqrt{2JU}$  quantum fluctuations dominate over thermal fluctuations. At  $T = 0$  and  $T^* = T_{KT} \sim J$  (with  $T_{KT}$  being the temperature of the Kosterlitz-Thouless transition in a  $2d$  XY model) quantum phase slips yield the superconductor-insulator transition.<sup>10-13</sup> The persistent currents in the quantum regime have been computed numerically for long chains,<sup>14,15</sup> as well as analytically using the effective low-energy description.<sup>16</sup>

Here we focus on the classical thermal regime corresponding to the temperature range  $T^* \ll T$ , which is easily accessible in experiment. We begin with analytical calculation of the low-temperature behavior of the persistent current  $I$  and the energy barrier for the phase slip. The numerical computation of the equilibrium value and dynamics of  $I$  that follows is challenging for two reasons. Firstly, while fluctuations of the current decrease with the length of the chain, so does the current itself,  $I \propto 1/N$ . Thus increasing the system size does not suppress fluctuations and an extensive averaging is needed. Secondly, accounting for the exponentially rare phase slips at  $T \ll J$  requires a very long computer time.

We propose an efficient numerical method to compute both equilibrium and dynamic properties.

## II. THE MODEL

The energy of the ring is a sum of charging energies of the grains with and the Josephson coupling energy (see, e.g. Ref. 15 and references therein)

$$\mathcal{H} = \sum_{i=1}^N \left\{ \frac{C}{2} V_i^2 + J \left[ 1 - \cos \left( \theta_{i+1} - \theta_i + \frac{2\pi\phi}{N} \right) \right] \right\}. \quad (1)$$

Here  $C$  is the capacitance of a superconducting grain with respect to the ground,  $V_i$  is the voltage of the  $i$ -th grain,  $\phi = \Phi/\Phi_0$  with  $\Phi$  being the magnetic flux piercing the ring and  $\Phi_0 = h/(2e)$  being the flux quantum. Using the Josephson relation

$$V_i = \frac{\hbar}{2e} \dot{\theta}_i, \quad (2)$$

where  $\theta_i$  is the phase of the superconducting order parameter of the  $i$ -th grain ( $\dot{\theta}_i = d\theta_i/dt$ ), one can rewrite the energy as

$$\mathcal{H} = \sum_{i=1}^N \left\{ \frac{\hbar^2}{4U} \dot{\theta}_i^2 + J \left[ 1 - \cos \left( \theta_{i+1} - \theta_i + \frac{2\pi\phi}{N} \right) \right] \right\} \quad (3)$$

with  $U \equiv E_C = 2e^2/C$ . Mechanical analogy to our problem is a chain of rotators with the moment of inertia  $\frac{\hbar^2}{2U}$ .

Due to periodicity of the ring, the sum rule  $\sum_{i=1}^N (\theta_{i+1} - \theta_i) = 2\pi m$  with  $m$  being an integer,  $0 \leq m \leq N-1$ , is satisfied. The limitation on  $m$  is similar to that on the wave vector in the Brillouin zone. For a given  $m$  the minimum of the Josephson energy is achieved when all phase differences are the same,  $\theta_{i+1} - \theta_i = 2\pi m/N$ :

$$E_J^{(m)} = NJ \left[ 1 - \cos \frac{2\pi(m + \phi)}{N} \right]. \quad (4)$$

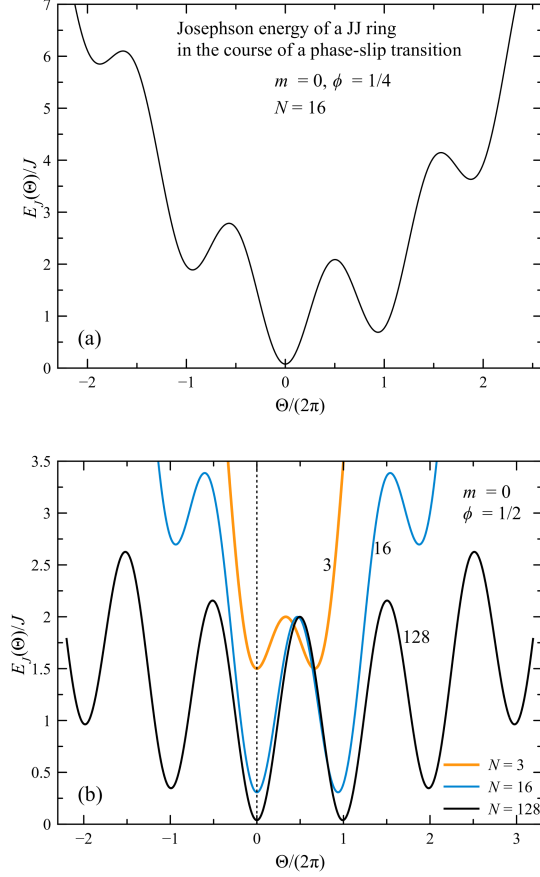


Figure 1: Josephson energy  $E_J$  vs the phase-slip angle  $\Theta$ , Eq. (6). (a)  $\phi = 1/4$ . (b)  $\phi = 1/2$ .

In the half-integer-fluxon case,  $\phi = n + 1/2$ , this ground state is degenerate,  $E_J^{(-n)} = E_J^{(-n-1)} = NJ(1 - \cos \frac{\pi}{N})$ . For  $0 < \phi < 1/2$  the ground and first excited states are  $m = 0, -1$ , their energy difference being

$$E_J^{(-1)} - E_J^{(0)} = 2NJ \sin \frac{\pi}{N} \sin \frac{\pi(1-2\phi)}{N}. \quad (5)$$

This and all other energy differences become small for large  $N$ .

Consider the energy barrier for a phase slip. To change  $m$  in a manner that requires minimum work, one has to change the phase difference  $\Theta$  between any pair of neighboring grains from nearly zero to nearly  $2\pi$ , keeping all other phase differences small and constant,  $\theta_{i+1} - \theta_i = \Delta\theta$ . Eliminating  $\Delta\theta$  from the periodicity condition  $\Theta + (N-1)\Delta\theta = 2\pi m$  yields the Josephson energy<sup>16</sup>

$$E_J(\Theta) = NJ - J \cos \left( \Theta + \frac{2\pi\phi}{N} \right) - (N-1)J \cos \left( \frac{2\pi m - \Theta}{N-1} + \frac{2\pi\phi}{N} \right) \quad (6)$$

shown in Fig. 1. For  $N \gg 1$  the second cosine becomes a parabola with superimposed oscillations due to the first

cosine. Transition from  $m$  to  $m' = m - \eta$  with  $\eta = \pm 1$  occurs via changing  $\Theta$  from  $\Theta^{(m)} = \Delta\theta^{(m)} = 2\pi m/N$  to  $\Theta^{(m')} = \Delta\theta^{(m')} + 2\pi\eta$ . Here from the periodicity condition in the form  $2\pi\eta + N\Delta\theta^{(m')} = 2\pi m$  one obtains  $\Delta\theta^{(m')} = 2\pi m'/N$ . In particular, transition from  $m = 0$  to  $m' = -1$  ( $\eta = 1$ ) requires the change in  $\Theta$  from zero to  $2\pi(1-1/N)$ . Analysis of  $E_J(\Theta)$  shows that for  $\phi = 1/2$  it is symmetric with the top of the energy barrier between the two minima at  $\Theta_b = \pi(1-1/N)$ , so that

$$B = E_J(\Theta_b) - E_J(0) = J \left[ 2 - N \left( 1 - \cos \frac{\pi}{N} \right) \right]. \quad (7)$$

The barrier varies from  $J/2$  at  $N = 3$  to  $2J$  at  $N \rightarrow \infty$ .

Classical equation of motion corresponding to Eq. (3) reads

$$\frac{\hbar^2}{2U} \ddot{\theta}_i = - \frac{\partial \mathcal{H}}{\partial \theta_i}. \quad (8)$$

In terms of grain charge  $Q_i = CV_i = \frac{e\hbar}{U} \dot{\theta}_i$  this becomes continuity equation

$$\dot{Q}_i = - \frac{2e}{\hbar} \frac{\partial \mathcal{H}}{\partial \theta_i} = - \frac{2\pi}{\Phi_0} \frac{\partial \mathcal{H}}{\partial \theta_i} = I_{i,i+1} + I_{i,i-1}, \quad (9)$$

where

$$I_{i,i\pm 1} = \frac{2\pi J}{\Phi_0} \sin \left( \theta_{i\pm 1} - \theta_i + \frac{2\pi\phi}{N} \right) \quad (10)$$

is the current flowing into grain  $i$  from grain  $i \pm 1$ . For the chain current in the direction of increasing  $i$  we will use the average

$$I = \frac{2\pi J}{\Phi_0} \frac{1}{N} \sum_{i=1}^N \sin \left( \theta_{i+1} - \theta_i + \frac{2\pi\phi}{N} \right). \quad (11)$$

This formula also can be obtained as  $I = \partial \mathcal{H} / \partial \Phi$ .

In terms of the dimensionless momenta  $p_i$  defined via  $\dot{\theta}_i = \frac{\sqrt{2JU}}{\hbar} p_i$ , the kinetic energy in Eq. (3) becomes  $E_k = \sum_i \frac{J}{2} p_i^2$ , and with the dimensionless time  $\tau = \frac{\sqrt{2JU}}{\hbar} t$  equations of motion become

$$\frac{dp_i}{d\tau} = \sin(\theta_{i+1} - \theta_i) + \sin(\theta_{i-1} - \theta_i), \quad \frac{d\theta_i}{d\tau} = p_i. \quad (12)$$

This system is equivalent to a closed chain of interacting rotators, with the charging energy playing the role of kinetic energy and the Josephson energy being potential energy. Here we study the limit of negligible dissipation which does not show up on the time scale of the experiment. We used Wolfram Mathematica with compilation in C. As the differential-equation solver we used the 5th order Butcher's Ruge-Kutta method that makes 6 function evaluations per integration step. High precision of this integrator allows using a larger integration step  $\Delta\tau = 0.2$ .

### III. EQUILIBRIUM PROPERTIES

To consider equilibrium properties analytically at low temperatures, it is convenient to introduce reduced phases  $\tilde{\theta}_i$  according to  $\theta_i = \tilde{\theta}_i + \frac{2\pi m}{N}(i-1)$  (so that accumulation of the reduced phases over the ring is zero). Thermal average of the ring's Josephson energy  $E_J \equiv \langle \mathcal{H}_J \rangle$  is given by<sup>15</sup>

$$\begin{aligned} E_J &= NJ \left[ 1 - \left\langle \cos \left( \tilde{\theta}_{i+1} - \tilde{\theta}_i + \frac{2\pi(\phi+m)}{N} \right) \right\rangle \right] \\ &= NJ \left[ 1 - \left\langle \cos \left( \frac{2\pi(\phi+m)}{N} \right) \right\rangle \left\langle \cos (\tilde{\theta}_{i+1} - \tilde{\theta}_i) \right\rangle \right], \end{aligned} \quad (13)$$

where we have taken into account  $\langle \sin (\tilde{\theta}_{i+1} - \tilde{\theta}_i) \rangle = 0$  and decoupled fluctuations of the winding number  $m$  and reduced phases  $\tilde{\theta}_i$ . The latter describe harmonic fluctuations that are similar to spin-wave theory for the equivalent system of the two-component classical spins. Thus one can use the known result for the  $XY$  classical spin chain in one dimension,

$$\langle \cos (\tilde{\theta}_{i+1} - \tilde{\theta}_i) \rangle = 1 - \frac{T}{2J}. \quad (14)$$

In a similar way, or just by  $I = \partial E_J / \partial \Phi$ , one obtains

$$I = \frac{2\pi J}{\Phi_0} \left\langle \sin \frac{2\pi(\phi+m)}{N} \right\rangle \left( 1 - \frac{T}{2J} \right). \quad (15)$$

At  $T \ll J$  phase slips changing  $m$  are exponentially rare, and one can discard averaging in Eq. (15). For  $\phi = 0$  the ground state is  $m = 0$ , and the corresponding current is zero. For  $\phi = 1/2$ , there are two opposite  $I$  values in the degenerate ground states  $m = 0, -1$ . Eq. (15) is valid within time intervals between rare phase slips  $0 \rightleftharpoons -1$ . However, the large-time average of  $I$  is zero. To the contrary, in non-degenerate cases, such as  $\phi = 1/4$ , there is a robust thermal average value of  $I$ .

At higher temperatures one has to take into account thermal fluctuations of  $m$  that are especially pronounced at large  $N$  since energy differences between states with different  $m$  decrease with  $N$  (see Fig. 1b). Averaging over  $m$  can be done by

$$I = \frac{2\pi J}{\Phi_0} \left( 1 - \frac{T}{2J} \right) \frac{1}{Z} \sum_{m=0}^{N-1} \sin \frac{2\pi(\phi+m)}{N} \exp \left( -\frac{E_J^{(m)}}{T} \right), \quad (16)$$

where  $Z$  is the corresponding partition function and

$$E_J^{(m)} = NJ \left[ 1 - \cos \left( \frac{2\pi(\phi+m)}{N} \right) \right] \left( 1 - \frac{T}{2J} \right), \quad (17)$$

c.f. Eq. (4). Harmonic corrections in this formula are important in the intermediate temperature range for  $N \gg 1$ , where  $m$ -fluctuations have to be taken into account but harmonic approximation still holds.

Equilibrium properties of the system can be computed either by the Monte Carlo (Metropolis) routine for effective two-component classical spins  $\mathbf{s}_i = (\sin \theta_i, \cos \theta_i)$ . Since at  $T \ll J$  equilibration of winding numbers  $m$  becomes very slow, standard Monte Carlo routine using trial changes of directions of individual spins fails to reach equilibrium. However, adding trial changes of  $m$  in the routine,

$$\theta_i \rightarrow \theta'_i \equiv \theta_i + \frac{2\pi m'(i-1)}{N}, \quad 0 \leq m' \leq N-1 \quad (18)$$

(one time before or after the full system update by individual rotations) makes the system equilibrate fast in spite of energy barriers shown in Fig. 1.

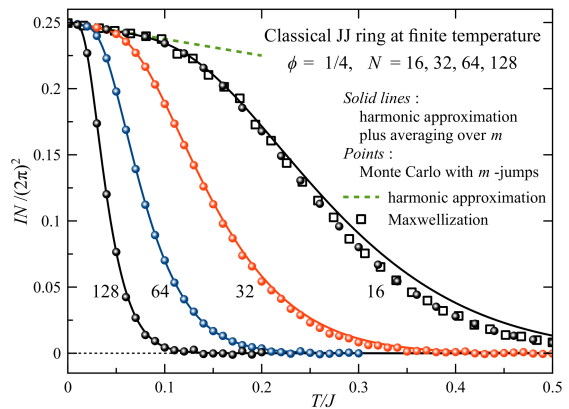


Figure 2: Thermal averages of the current at  $\phi = 1/4$  for different  $N$ . Numerical results (symbols) are obtained by Monte Carlo with  $m$ -jumps and analytical results (solid lines) are those of Eq. (16). Dashed line is harmonic approximation, Eq. (15) without angular brackets and with  $m = 0$ .

Thermal equilibrium values of the current for different numbers of grains in the ring are shown in Fig. 2, setting  $J = \Phi_0 = 1$ . Most of the numerical data were obtained by Monte Carlo with trial  $m$ -jumps added, that allows to reach equilibrium at any temperature. Analytical results of Eq. (16) are in accordance with numerical data. In experiment it can be difficult to reach equilibrium at low temperatures because of energy barriers. The required equilibration time can be estimated using our dynamical results below.

### IV. MAXWELLIZATION METHOD FOR THERMODYNAMICS AND EQUILIBRIUM DYNAMICS

While Monte Carlo is a mainstream method at equilibrium, it is not suitable for dynamical problems simply because it is not based on real dynamics. We propose here another numerical method for statics and equilibrium dynamics of classical systems having kinetic energy, such as

arrays of Josephson junctions. In this method that we call *maxwellization*, equations of motion, here Eq. (12), are solved numerically over a long time interval  $(0, \tau_{\max})$  divided into sub-intervals of length  $\tau_0 \ll \tau_{\max}$ . At the end of each sub-interval the momenta  $p_i$ , having the Maxwell distribution  $f_p \propto \exp\left(-\frac{Jp^2}{2T}\right)$  with the average kinetic energy  $T/2$  per particle at equilibrium, are generated anew with another realization of the Maxwell distribution at the same temperature  $T$ , leaving the phases  $\theta_i$  unchanged. In such a way a statistical ensemble is created in which the energy of the system is fluctuating. Kinetic energy is converted into potential energy during the microscopic time  $\tau \sim 1$ , thus the whole system becomes quickly thermalized. After a short thermalization time, one can begin measuring physical quantities by averaging the solution of the equations of motion over large times. Maxwellization method works for both equilibrium and dynamic problems. We have checked that maxwellization yields the same results with  $\tau_0 \sim 1$  and  $\tau_0 \gg 1$ . Fig. 3 shows that thermal Josephson energies  $E_J$  obtained by Monte Carlo are the same as obtained by maxwellization, the accuracy and computer time being comparable.

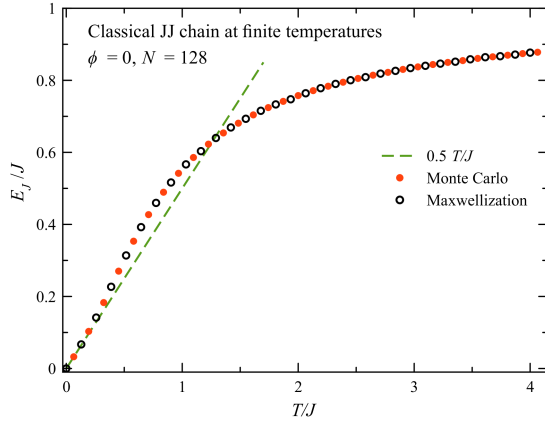


Figure 3: Josephson energies  $E_J$  vs  $T$ , obtained by Monte Carlo and by maxwellization.

Maxwellization results are also shown in Fig. 2 for  $N = 16$  with  $\tau_{\max} = 10^8$ . For larger  $N$  maxwellization cannot reach equilibrium, similar to standard Monte Carlo without  $m$ -jumps. Unlike Monte Carlo, maxwellization cannot be extended to include  $m$ -jumps since it is based on the realistic dynamics.

The background for the application of the maxwellization method to equilibrium dynamics is the following. Dynamics of underdamped systems of many superconducting grains that are considered throughout this paper is predominantly internal and it is non-trivial enough to generate phase slips. Small coupling to the bath only slightly perturbs the dynamics and can be neglected. The system serves as a bath for itself. In the underdamped case one can use the microcanonical approach and average the energy-dependent phase-slip rate  $\Gamma(E)$ , obtained

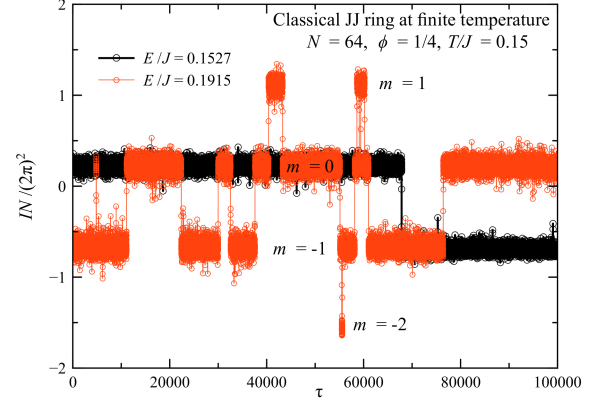


Figure 4: Time dependence of the current at  $\phi = 1/4$ , showing harmonic fluctuations and phase slips in states with two different total energies  $E$ , generated at the same  $T$ .

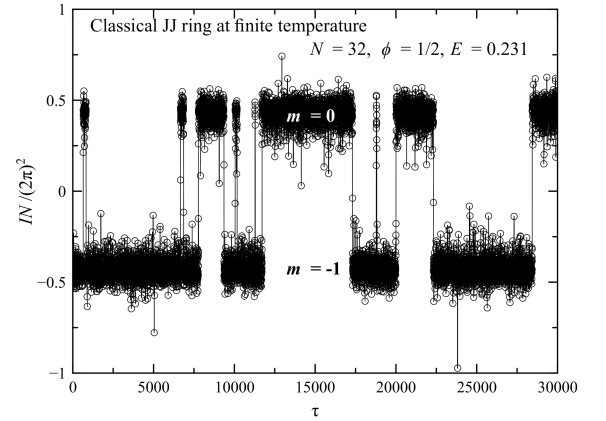


Figure 5: Time dependence of the Josephson current at  $\phi = 1/2$ , showing harmonic fluctuations and phase slips.

for the isolated system as explained in the next section, over the energies satisfying the Gibbs distribution as follows

$$\Gamma(T) = \frac{1}{Z} \int dE \rho(E) e^{-E/T} \Gamma(E). \quad (19)$$

Here  $Z$  is partition function and  $\rho(E)$  is the density of states of the system, while  $E$  is energy per grain above the ground-state energy.  $\Gamma(E)$  vanishes for  $E < B/N$ , where  $B$  is given by Eq. (7). For  $N \gg 1$  the system is above the barrier in a wide range of energies  $E$  and can cross the barrier via its internal dynamics without any help of the bath. Practically, instead of integrating with the poorly-known  $\rho(E)$ , one can sample energy states with the help of the Monte Carlo procedure for phases  $\theta_i$  and Maxwell distribution for their time derivatives  $\dot{\theta}_i$  (both being statistically independent for classical

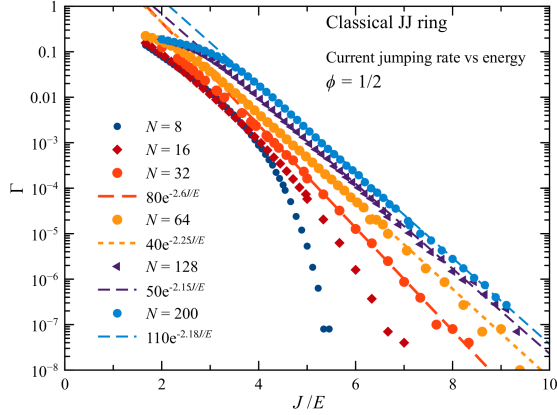


Figure 6: Microcanonical superconducting current transition rate  $\Gamma(E)$  of a ring of  $N$  Josephson junctions in the half-fluxon case.

systems), that is

$$\Gamma(T) = \frac{1}{N_{\text{samp}}} \sum_{i=1}^{N_{\text{samp}}} \Gamma(E_i), \quad (20)$$

where  $N_{\text{samp}}$  is the number of sampled states that has to be large, especially at low temperatures.

The microcanonical method was applied at the early stages of the work and it gave the results perfectly consistent with those obtained by the maxwellization that is nothing else than its computational improvement. The computational difficulty with the microcanonical method is that at low energies  $\Gamma(E)$  is very small and one needs to run conservative dynamics over very large time intervals to have a few phase slips. The numerical integration method should be very accurate to avoid energy drift that will spoil the results. In fact, in the present computations energy corrections were introduced to ensure conservation of the energy. To compute  $\Gamma(T)$ , the best strategy is to pre-compute  $\Gamma(E)$  over a relevant range of energies, build an interpolation function over these results, and then run Monte Carlo for Eq. (20).

The microcanonical method is working well and it could be used as the main method in this project. However, the maxwellization method is more direct, robust, and elegant. This method puts dynamics and statistics into one. There is only one very long dynamical run, in the course of which kinetic energies are re-assigned according to the Maxwell distribution at regular intervals  $\tau_0 \ll \tau_{\text{max}}$ . In this way, the statistical ensemble is being built during the evolution of the system, closer to what happens in reality. One does not need to strictly ensure energy conservation in the numerical integration of the equations of motion since the energy is changing anyway. Results of the maxwellization method do not depend on  $\tau_0$  and are exactly the same as those obtained by the microcanonical method.

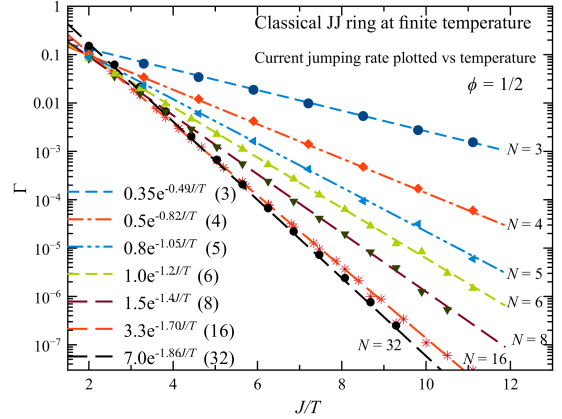


Figure 7: Numerically computed transition rates  $\Gamma$  with Arrhenius fits for transitions between opposite directions of the current, corresponding to  $m = 0$  and  $m = -1$ , for rings of different length in the half-fluxon case.

## V. DYNAMICS OF PHASE SLIPS: NUMERICAL RESULTS

Typical time dependences of  $I$  obtained by solving the equation of motion, Eq. (12), and using Eq. (11) for a quarter-fluxon threading the ring are shown in Fig. 4 in states with two different dynamically conserved energies, generated at the same temperature. In this illustrative computation, no maxwellization has been done to show that fluctuations of the current have mainly dynamic origin. Jumps correspond to the transitions (phase slips) between different values of  $m$  indicated in the figure. Small fluctuations between phase slips are harmonic excitations. Dynamical fluctuations of  $I$  are stronger in the states with a higher energy. Due to the lack of symmetry (see Fig. 1a), there is a non-zero time average of the current, shown in Fig. 2 as the maxwellization result for  $N = 16$ .

In the half-fluxon case the energy is degenerate and the current averaged over long times is always zero.  $I(\tau)$  exhibits jumps between opposite directions corresponding to  $m = 0$  and  $m = -1$ , on top of harmonic fluctuations around these states, see Fig. 5 (also without maxwellization). The rate of transitions between the opposite values of  $I$  can be computed as  $\Gamma = N_{\text{jumps}}/\tau_{\text{max}}$ , where  $N_{\text{jumps}}$  is the number of current jumps within the time interval of length  $t_{\text{max}}$ .

Transition rate  $\Gamma(E)$  obtained from the conservative evolution of the system is shown in Fig. 6. For large  $N$  the results can be fitted with the Arrhenius energy dependence. For smaller  $N$ , the curves deviate downwards from straight lines since  $\Gamma(E) = 0$  for  $E < B/N$ , as argued above. These results can be used to obtain  $\Gamma(T)$  by statistical sampling at the temperature  $T$ , see Eq. (20). The results are in agreement with the results obtained by the maxwellization.



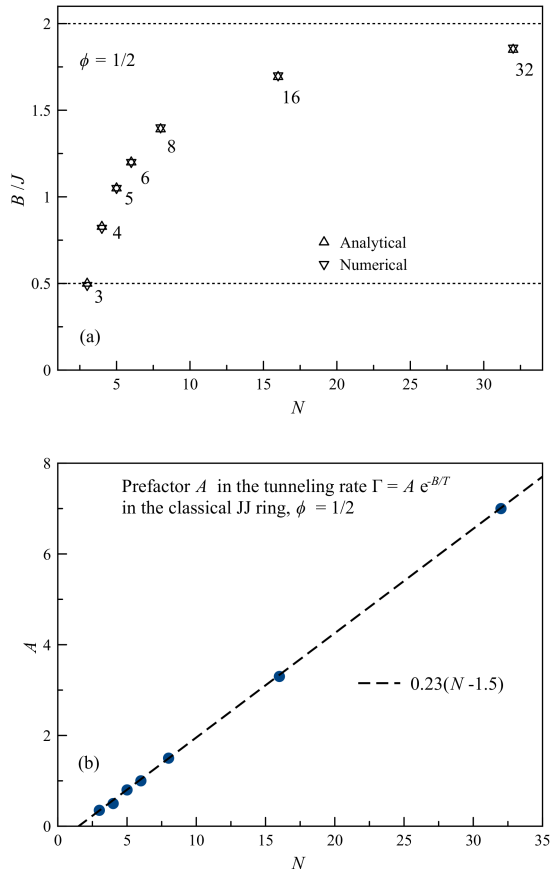


Figure 8: Thermal fluctuations of  $I$  at a half fluxon. (a) Barrier energies  $B$  extracted from the fits of  $\Gamma$  in Fig. 7, compared to their analytical values from Eq. (7). (b) Prefactor  $A$  extracted from numerical data.

The results for  $\Gamma(T)$  obtained directly by the maxwellization, as explained in the preceding section, follows the law  $\Gamma = A \exp(-B/T)$ . This is shown for closed chains of different length in Fig. 7 (in terms of the dimensionless time  $\tau$  with  $\tau_{\max} = 10^8$ ). Numerically obtained exponents  $B(N)$  are in excellent agreement with the analytical result given by Eq. (7), as one can see from Fig. 8. The computed prefactor is well approximated by

$A = 0.23(N - 3/2)$ . Its proportionality to  $N$  at large  $N$  agrees with the fact that the phase slip can occur at any of the  $N$  sites of the chain. At higher temperatures,  $T \sim J$ , temporal behavior of the current becomes more chaotic as it involves transitions between other values of  $m$  as well.

## VI. DISCUSSION

We have considered equilibrium and dynamic properties of Josephson-junction rings in the classical limit. It was shown that for rings composed of many junctions,  $N \gg 1$ , one has to take into account different values of the winding number  $m$  in the thermodynamics of the persistent current caused by the magnetic flux piercing the ring. Analytical results combining harmonic approximation with averaging over different  $m$  have been confirmed by a Monte Carlo routine allowing  $m$ -jumps (phase slips). Energy barriers for phase slips have been obtained analytically and shown to increase with  $N$ .

Numerical method of “maxwellization” for solving thermodynamic and equilibrium dynamic problems has been developed and applied to JJ rings. This method is based on real dynamics and it is suitable for computation of quantities such as transition rates at a given temperature. In particular, we have obtained Arrhenius temperature dependence of the inversion rate of the persistent current at a half fluxon with the barrier given by our analytical expressions.

By visualizing the temporal behavior of the current in Josephson junction chains, our results provide guidance for future experiments in this field. Similar numerical approach can be tried to study open chains with a bias current.

## Acknowledgments

This work has been supported by the grant No. DE-FG02-93ER45487 funded by the U.S. Department of Energy, Office of Science.

- <sup>1</sup> See, e.g., G. Schwiete and Y. Oreg, Persistent current in small superconducting rings, *Physical Review Letters* **103**, 037001-(4) (2009), and references therein.
- <sup>2</sup> See review and references therein: J. E. Mooij, G. Schön, A. Shnirman, T. Fuse, C. J. P. M. Harmans, H. Rotzinger, and A. H. Verbruggen, Superconductor-insulator transition in nanowires and nanowire arrays, *New Journal of Physics* **17**, 033006-(12) (2015).
- <sup>3</sup> I. M. Pop, I. Protopopov, F. Lecocq, Z. Peng, B. Pannetier, O. Buisson, and W. Guichard, Measurement of the effect of quantum phase-slips in a Josephson junction chain, *Nature*

*Physics* **6**, 589-592 (2010).

- <sup>4</sup> K. A. Matveev, A. I. Larkin, and L. I. Glazman, Persistent current in superconducting nanorings, *Physical Review Letters* **89**, 096802-(4) (2002).
- <sup>5</sup> M. Y. Choi, Persistent current and voltage in a ring of Josephson junctions, *Physical Review B* **48**, 15920-15925 (1993).
- <sup>6</sup> R. M. Bradley and S. Doniach, Quantum fluctuations in chains of Josephson junctions, *Physical Review B* **30**, 1138-1147 (1984).
- <sup>7</sup> M. Wallin, E. S. Sørensen, S. M. Girvin, and A. P. Young,

- Superconductor-insulator transition in two-dimensional dirty boson systems, *Physical Review B* **49**, 12115-12139 (1994).
- <sup>8</sup> See, e.g., S. L. Sondhi, S. M. Girvin, J. P. Carini, and D. Shahar, Continuous quantum phase transitions, *Review of Modern Physics* **69**, 315-333 (1997).
- <sup>9</sup> S. Sachdev, *Quantum Phase Transitions* (Cambridge University Press, Cambridge, UK, 2011).
- <sup>10</sup> A. D. Zaikin, D. S. Golubev, A. van Otterlo, and G. T. Zimanyi, Quantum phase slips and transport in ultrathin superconducting wires, *Physical Review Letters* **78**, 1552-1555 (1997).
- <sup>11</sup> D. S. Golubev and A. D. Zaikin, Quantum tunneling of the order parameter in superconducting nanowires, *Physical Review B* **64**, 014504-(14) (2001).
- <sup>12</sup> S. E. Korshunov, Effect of dissipation on the low-temperature properties of a tunnel-junction chain, *Soviet Physics JETP* **68**, 609-618 (1989).
- <sup>13</sup> E. Chow, P. Delsing, and D. B. Haviland, Length-scale dependence of the superconductor-to-insulator quantum phase transition in one dimension. *Physical Review Letters* **81**, 204-207 (1998).
- <sup>14</sup> M. Lee, M.-S. Choi, and M. Y. Choi, Quantum phase transitions and persistent currents in Josephson-junction ladders, *Physical Review B* **68**, 144506-(11) (2003).
- <sup>15</sup> D. A. Garanin and E. M. Chudnovsky, Quantum decay of the persistent current in a Josephson junction ring, *Physical Review B* **93**, 094506-(9) (2016).
- <sup>16</sup> G. Rastelli, I. M. Pop, and F. W. J. Hekking, Quantum phase-slips in Josephson junction rings, *Physical Review B* **87**, 174513-(18) (2013).